# Self-Assembled Monolayer of Polyoxometalate on Gold Surfaces: Quartz Crystal Microbalance, Electrochemistry, and in-Situ Scanning Tunneling Microscopy Study

Zhiyong Tang, Shaoqin Liu, Erkang Wang,* and Shaojun Dong*

*Laboratory of Electroanalytical Chemistry, and National Analytical Research Center of Electrochemistry and Spectroscopy, Changchun Institute of Applied Chemistry, Chinese Academy of Sciences, Changchun 130022, P. R. China*

*Received June 4, 1999. In Final Form: December 28, 1999*

A new kind of inorganic self-assembled monolayer (SAM) was prepared by spontaneous adsorption of polyoxometalate anion, $AsMo_{11}VO_{40}^{4-}$, onto a gold surface from acidic aqueous solution. The adsorption process, structure, and electrochemical properties of the $AsMo_{11}VO_{40}^{4-}$ SAM were investigated by quartz crystal microbalance (QCM), electrochemistry, and scanning tunneling microscopy (STM). The QCM data suggested that the self-assembling process could be described in terms of the Langmuir adsorption model, providing the value of the free energy of adsorption at −20 KJ $mol^{-1}$. The maximum surface coverage of the $AsMo_{11}VO_{40}^{4-}$ SAM on gold surface was determined from the QCM data to be $1.7 \times 10^{-10}$ mol $cm^{-2}$, corresponding to a close-packed monolayer of $AsMo_{11}VO_{40}^{4-}$ anion. The analysis of the voltammograms of the $AsMo_{11}VO_{40}^{4-}$ SAM on gold electrode showed three pairs of reversible peaks with an equal surface coverage of $1.78 \times 10^{-10}$ mol $cm^{-2}$ for each of the peaks, and the value was agreed well with the QCM data. In-situ STM image demonstrated that the $AsMo_{11}VO_{40}^{4-}$ SAM was very uniform and no aggregates or multilayer could be observed. Furthermore, the high-resolution STM images revealed that the $AsMo_{11}VO_{40}^{4-}$ SAM on Au(111) surface was composed of square unit cells with a lattice space of 10−11 Å at +0.7 V (vs Ag|AgCl). The value was quite close to the diameter of $AsMo_{11}VO_{40}^{4-}$ anion obtained from X-ray crystallographic study. The surface coverage of the $AsMo_{11}VO_{40}^{4-}$ SAM on gold electrode estimated from the STM image was around $1.8 \times 10^{-10}$ mol $cm^{-2}$, which was consistent with the QCM and electrochemical results.

## Introduction

The self-assembled organic monolayer chemistry has been paid intensive attention in the past 20 years, since Sagiv reported that alkanesilanes could be used to form a stable monolayer on glass or aluminum oxides.[1,2] Outstanding work on the synthesis and characterization of alkanethiol/gold self-assembled monolayers (SAMs) was conducted by Whitesides,[3−8] Nuzzo,[9−15] Allara,[12−16] and Chidsey et al.[16−18] The chemistry of SAMs provides an opportunity to control the film structure at the molecular level and enables tailoring of the surface properties through incorporation of various organic functional groups into the adsorbate molecules.[19,20] Although organic SAMs have been found to have potential utility in sensors,[21,22] submicrometer lithographic patterning schemes,[23,24] and molecular electronic demonstrations,[25,26] many undesirable features, such as their oxidization on exposure to air,[27−29] instability in the typical thermal conditions,[30−33] and desorption in organic solvents,[34−36] preclude the practical use of the organic SAMs.

* To whom correspondence should be addressed. Fax: +86-431-5687911. E-mail: ekwang@mail.jlu.edu.cn.

(1) Sagiv, J. *Irsr. J. Chem.* **1979**, *18*, 339.
(2) Sagiv, J. *J. Am. Chem. Soc.* **1980**, *102*, 2.
(3) Bain, C. D.; Whitesides, G. M. *J. Am. Chem. Soc.* **1988**, *110*, 3665.
(4) Bain, C. D.; Whitesides, G. M. *J. Am. Chem. Soc.* **1988**, *110*, 5897.
(5) Bain, C. D.; Whitesides, G. M. *J. Am. Chem. Soc.* **1988**, *110*, 6560.
(6) Bain, C. D.; Whitesides, G. M. *Science* **1988**, *240*, 62.
(7) Bain, C. D.; Evall, J.; Whitesides, G. M. *J. Am. Chem. Soc.* **1989**, *111*, 7155.
(8) Biebukyck, H. A.; Whitesides, G. M. *Langmuir* **1993**, *9*, 1766.
(9) Nuzzo, R. G.; Zegarski, B. R.; Dubois, L. H. *J. Am. Chem. Soc.* **1987**, *112*, 570.
(10) Dubois, L. H.; Zegarski, B. R.; Nuzzo, R. G. *J. Am. Chem. Soc.* **1990**, *112*, 570.
(11) Dubois, L. H.; Zegarski, B. R.; Nuzzo, R. G. *Annu. Rev. Phys. Chem.* **1992**, *43*, 437.
(12) Nuzzo, R. G.; Allara, D. L. *J. Am. Chem. Soc.* **1983**, *105*, 4481.
(13) Nuzzo, R. G.; Fusco, F. A.; Allara, D. L. *J. Am. Chem. Soc.* **1987**, *109*, 2358.
(14) Nuzzo, R. G.; Dubois, L. H.; Allara, D. L. *J. Am. Chem. Soc.* **1990**, *112*, 558.
(15) Allara, D. L.; Nuzzo, R. G. U.S. Patent Application 389,775, June 18, 1982; U.S. Patent 4,690,715, Sept 1, 1987 .
(16) Porter, M. D.; Bright, T. B.; Allara, D. L.; Chidsey, C. E. D. *J. Am. Chem. Soc.* **1987**, *109*, 3559.
(17) Chidsey, C. E. D.; Bertozzi, C. R.; Putvinski, T. M.; Mujsece, A. M. *J. Am. Chem. Soc.* **1990**, *112*, 4301.
(18) Chidsey, C. E. D. *Science* **1991**, *251*, 919.
(19) Finklea, H. O. In *Electroanalytical Chemistry*; Bard, A. J., Rubinstein, I., Eds.; Marcel Dekker: New York, 1996; Vol. 19, p 109.
(20) Bain, C. D.; Evans, S. D. *Chem. Br.* **1995**, *31*, 46.
(21) Ricco, A. J.; Kepley, L. J.; Thomas, R. C.; Sun, L.; Crooks, R. M. *Technical Digest Series*; IEEE solid-state Sensor and Actutor Workshop, Hilton Head Island, SC; IEEE: Piscataway, NJ, 1992, 114.
(22) Pevzner, P. A.; Lipshutz, R. J. *Proceedings of Mathmetical Foundations of Computer Science*; 19th International Symposium, Slovakia; Springer-Verlag: Berlin, Germany, 1994; p 143.
(23) Sondag-Huethorst, J. A.; Helleputte, H. R. J. V.; Fokkink, L. G. J. *Appl. Phys. Lett.* **1994**, *64*, 285.
(24) Lercel, M. J.; Craighead, H. G.; Paikh, A. N.; Seshadri, K. Allara, D. L. J. *Appl. Phys. Lett.* **1996**, *68*, 1504.
(25) Bumm, L. A.; Arnold, J. J.; Cygn, M. T.; Dunbar, T. D.; Burgin, T. P.; Jones, L.; Allara, D. L.; Tour, J. M.; Weiss, P. S. *Science* **1996**, *271*, 1705.
(26) Feldheim, D. L.; Keating, C. D. *Chem. Soc. Rev.* **1998**, *27*, 1.
(27) Li, Y.; Huang, J.; Mclver, R. T.; Hemminger, J. C. *J. Am. Chem. Soc.* **1992**, *114*, 2428.
(28) Chadwick, J. E.; Myles, D. C.; Garrel, R. L. *J. Am. Chem. Soc.* **1993**, *115*, 10364.
(29) Garrell, R. L.; Chadwick, J. E.; Severence, D. L.; McDonald, N. A.; Myles, D. C. *J. Am. Chem. Soc.* **1995**, *117*, 11563.
(30) Nuzzo, R. G.; Zegarski, B. R.; Dubois, L. H. *J. Am. Chem. Soc.* **1987**, *109*, 733.
(31) Hickman, J. L.; Ofer, D.; Zou, C.; Wrighton, M. S.; Laibinis, P. E.; Whitesides, G. M. *J. Am. Chem. Soc.* **1991**, *113*, 1128.
(32) Jaffey, D. M.; Madix, R. J. *J. Am. Chem. Soc.* **1994**, *116*, 3012.
(33) Schlenoff, J. B.; Li, M.; Ly, H. *J. Am. Chem. Soc.* **1995**, *117*, 12528.

10.1021/la9907127 CCC: $19.00 
Published on Web 04/27/2000

Self-assembled inorganic monolayers will probably enjoy the popularity of the organic SAMs, due to the superior stability and mechanical properties of inorganic monolayers. Although much work on the adsorption of simple anions such as iodide,[37−39] bromide,[40,41] cyanide,[42,43] and sulfate/bisulfate[44−47] has been done, just recently pioneering studies on the SAMs of inorganic complexes have just been completed.[48−53] Polyoxometalates with well-defined primary structures are recently attracting much attention as building units of novel inorganic materials that may be useful in catalysis,[54,55] medicine,[56] biology,[57] and devices.[58−60] Especially, the polyoxometalate SAM on a carbon surface was obtained by Nadjo's and Barteau's groups through the method of solvent casting. In the present work the polyoxometalate anion, $AsMo_{11}VO_{40}^{4-}$, was used to fabricate the inorganic SAMs by spontaneous adsorption of $AsMo_{11}VO_{40}^{4-}$ anions on gold surface from acidic aqueous solution. The formation process and structure and properties of the inorganic SAMs were studied in detail by QCM, in-situ STM, and electrochemistry. The results demonstrate that the $AsMo_{11}VO_{40}^{4-}$ SAMs prepared have high stability and good electrochemical response. The new kind of SAM gives a substantial way for fabricating a self-assembled functional surface with high stability.

## Experimental Section

**1. Chemicals.** $H_4AsMo_{11}VO_{40}\cdot 18H_2O$ was synthesized by Professor Enbo Wang (Department of Chemistry, Northeast Normal University). Briefly, 280 mL of aqueous solution of sodium molybdate ($Na_2MoO_4\cdot 2H_2O$, 133 g) was adjusted to pH = 3.5 by adding $HClO_4$, and then the solution was directly poured into 30 mL of aqueous solution containing sodium hydrogen arsenate ($Na_2HAsO_4\cdot 7H_2O$, 15.7 g) and sodium vanadate ($NaVO_3\cdot 2H_2O$, 8 g) with stirring. The pH of mixture was adjusted with $HClO_4$ to −0.8 and continuously stirred for 1 h. After an insoluble substance was filtered, the solution was extracted by ether. Red 11-molybdovanadoarsenate solid was collected after ether volatilization. Finally, the 11-molybdovanadoarsenate crystals ($H_4AsMo_{11}VO_{40}\cdot 18H_2O$) were obtained by recrystallizing twice from pure water. The elemental analysis and spectral data of $H_4AsMo_{11}VO_{40}\cdot 18H_2O$ were in agreement with the proposed chemical structure. Experimental: As 3.48%, Mo 49.21%, V 2.37%, H 1.86%. Calculated: As 3.49%, Mo 49.10%, V 2.37%, H 1.88%. IR (2% KBr): 887.9 ($\nu_{As-Oa}$), 973.3 ($V_{Mo-Od}$), 773 ($V_{Mo-Oc-Mo}$) and 1614.7, 3349, 3449 ($V_{OH}$) ($cm^{-1}$). UV (200−400 nm, in $H_2O$): 210 and 317 nm. $^{51}V$ NMR (9 mM solution in $H_2O$; $D_2O$ in capillary insert): one resonance for V atom at 32.192.

All other reagents were of analytical grade and were used without further purification. Pure water was obtained by passing it through a Millipore Milli-Q water purification system. Electrolyte solutions were prepared by using $HClO_4$ (70 wt %, Fluka, p.a. grade). Before measurements, the solution was deaerated by passing purified Ar gas through the solution for at least 10 min.

**2. Quartz Crystal Microbalance (QCM).** QCM measurements were done by a QCM analyzer (Wuhan University, China). The quartz crystals used were covered by vapor-deposited gold electrodes on both faces. The resonance frequency was 9 MHz (AT-cut). The mass change, $\Delta m$, was estimated from the frequency shift, $\Delta F$, by using the Sauerbrey equation:[61,62]

$$\Delta F = -km \qquad (1)$$

Where the sensitivity factor ($k = -0.178$ Hz $cm^{-2}$ $ng^{-1}$) was estimated by means of silver electrodepositon.[63] Prior to each experiment, the gold electrode was treated with 0.1 M NaOH and 0.1 M $HClO_4$ successively and rinsed thoroughly with pure water.

**3. Electrochemical Experiments.** Electrochemical experiments were carried out on CH Instruments (model 600 Voltammetric analyzer) in a conventional one-compartment cell with a gold disk electrode (a diameter of 0.8 mm) as a working electrode, a Ag|AgCl (saturated with KCl) electrode as reference electrode, and a Pt electrode as counter electrode. The gold electrode was successively polished with 1.0, 0.3, and 0.05 $\mu$m $\alpha$-$Al_2O_3$ and washed ultrasonically with ethanol and water for each new experiment. Before self-assembly the gold electrode was treated with 0.1 M NaOH and 0.1 M $HClO_4$ and rinsed thoroughly with pure water. The real electrode surface area was estimated from the same cyclic voltammogram by integration of a cathodic peak for the reduction of an oxide layer performed electrochemically on the electrode surface,[64] and a roughness factor of $\sim 1.2 \pm 0.1$ was obtained for the gold electrode.

**4. In-Situ Scanning Tunneling Microscopy (STM).** For in-situ STM observation, Au single-crystal beads were prepared at the end of Au wires (99.99% purity) by the method of Clavilier et al.[65] The well-prepared Au bead consisted of (111) facets in an octahedral configuration. These (111) facets usually gave well-defined terrace and step structures. One of the (111) facets was directly used as a STM scanning plane. STM images were obtained with a Nanoscope IIIA scanning probe microscopy (Digital Instruments). The tunneling tip was made from an electrochemical etched tungsten wire with a diameter of 0.25 mm and sealed with a clear nail polish to minimize the faradic current. Platinum wires were used as the quasi-reference and counter electrodes during the electrochemical measurements.

(34) Groat, K. A.; Creager, S. E. *Langmuir* **1993**, *9*, 3668.
(35) Curtin, L. S.; Peck, S. R.; Tender, L. M.; Murray, R. W.; Rowe, G. K.; Creager, S. E. *Anal. Chem.* **1993**, *65*, 365.
(36) Ravenscroft, M. S.; Finklea, H. O. *J. Phys. Chem.* **1994**, *98*, 3843.
(37) Schardt, B. C.; Yau, S. L.; Rinaldi, F. *Sicence* **1989**, *243*, 1050.
(38) Yau, S. L.; Vitus, C. M.; Schardt, B. C. *J. Am. Chem. Soc.* **1990**, *112*, 3677.
(39) Gao, X.; Weaver, M. J. *J. Am. Chem. Soc.* **1992**, *114*, 8544.
(40) Lucas, C. A.; Markovic, N. M.; Ross, P. N. *Surf. Sci. Lett.* **1995**, *340*, L949.
(41) Orts, J. M.; Gomez, R.; Feliu, J. M.; Aldaz, A.; Clavilier, J. *Langmuir* **1997**, *13*, 3016.
(42) Stuhlmann, C.; Villegas, I.; Weaver, M. J. *Chem. Phys. Lett.* **1994**, *219*, 319.
(43) Kim, Y. G.; Yau, S.-L.; Itaya, K. *J. Am. Chem. Soc.* **1996**, *118*, 393.
(44) Magnussen, O. M.; Hagebock, J.; Hotlos, J.; Behm, R. J. *Faraday Discuss.* **1992**, *94*, 329.
(45) Funtikov, A. M.; Linke, U.; Stimming, U.; Vogel, R. *Surf. Sci. Lett.* **1995**, *324*, L343.
(46) Funtikov, A. M.; Stimming, U.; Vogel, R. *J. Electroanal. Chem.* **1997**, *428*, 147.
(47) Wan, L.-J.; Yau, S.-L.; Itaya, K. *J. Phys. Chem.* **1995**, *99*, 9507.
(48) Ge, M.; Zhong, B.; Klemperer, W. G.; Gewirth, A. A. *J. Am. Chem. Soc.* **1996**, *118*, 5812.
(49) Ge, M.; Niece, B. K.; Wall, G. G.; Klemperer, W. G.; Gewirth, A. A. *Mater. Res. Soc. Symp. Proc.* **1997**, *451*, 99.
(50) Ge, M.; Gewirth, A. A.; Klemperer, W. G.; Wall, G. G. *Pure Appl. Chem.* **1997**, *69*, 2175.
(51) Yeager, L. J.; Saeki, F.; Hawthorne, M. F.; Garrell, R. L. *J. Am. Chem. Soc.* **1998**, *120*, 9961.
(52) Keita, B.; Nadjo, L.; Kjoller, K. *Surf. Sci.* **1991**, *256*, L613.
(53) Watson, B. A.; Barteau, M. A.; Haggerty, L.; Lenhoff, A. M.; Weber, R. S. *Langmuir* **1992**, *8*, 1145.
(54) Misono, M. *Catal. Rev. Sci. Eng.* **1987**, *29*, 269.
(55) Watzenberger, A.; Emig, G.; Lynch, D. T. *J. Catal.* **1990**, *124*, 247.
(56) Bussereau, F.; Picard, M.; Malik, C.; Teze, A.; Blancou, J. *Ann. Inst. Pasteur/Virol.* **1988**, *32*, 33.
(57) Ono, K.; Nakane, H.; Barre-Sinoussi, F.; Chermann, C. *Nucleic Acids Res. Symp. Ser.* **1984**, *15*, 169.
(58) Pope, M. T. *Heteropoly and Isopoly Oxometalates*; Springer-Verlag: Berlin, 1983.
(59) Pope, M. T.; Muller, A. *Angew. Chem., Int. Ed. Engl.* **1991**, *30*, 34.
(60) Pope, M. T.; Muller, A. *Polyoxometalates: From Platonic Solid to Antiretroviral Activity*; Kluwer: Dordrecht, Nerthlands, 1994.
(61) Suerbrey, G. Z. *Z. Phys.* **1959**, *155*, 206.
(62) Buttry, D. A.; Ward, M. D. *Chem. Rev.* **1992**, *92*, 1355.
(63) Bruckenstein, S.; Swathirajan, S. *Electrochim. Acta* **1985**, *30*, 851.
(64) Finklea, H. O.; Henslew, D. D. *J. Electroanal. Chem.* **1993**, *347*, 327.
(65) Clavilier, J.; Armand, D.; Wu, B. L. *J. Electroanal. Chem.* **1982**, *135*, 159.

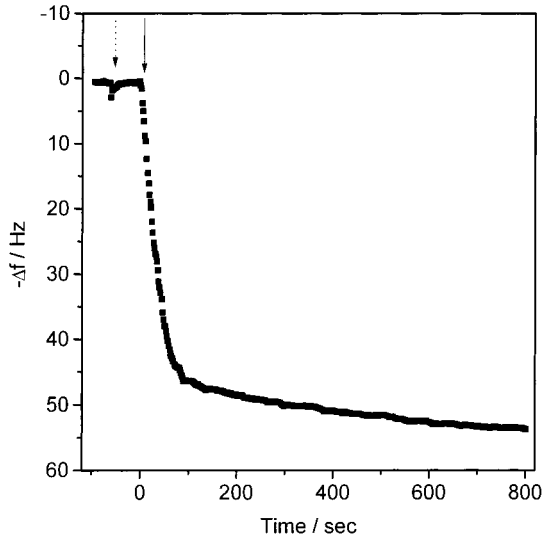


**Figure 1.** Frequency change versus time during the self-assembling of $AsMo_{11}VO_{40}^{4-}$ anion on an Au surface of QCM: injection of $AsMo_{11}VO_{40}^{4-}$ solution (solid arrow) following the injection of 0.1 M blank $HClO_4$ solution (dotted arrow).

Large-scale images shown here were taken in the constant-current mode. High-resolution images were obtained in the constant-height mode.

## Results and Discussion

**1. The Self-Assembling Process of $AsMo_{11}VO_{40}^{4-}$ Anion on Gold Surface.** The self-assembling process of $AsMo_{11}VO_{40}^{4-}$ in an argon-degassed and stirred 0.1 M $HClO_4$ solution on gold surface was monitored in situ by a QCM sensor. After the QCM stability of ±0.5 Hz in 0.1 M $HClO_4$ solution was achieved, the $AsMo_{11}VO_{40}^{4-}$ anion in 0.1 M $HClO_4$ solution was added, and the frequency change was recorded as shown in Figure 1. The resonant frequency decreases readily at the beginning (90% of the maximum $\Delta f$ decrease is obtained in 100 s) and then gradually attains a constant value, which implies that the adsorption of $AsMo_{11}VO_{40}^{4-}$ anion on gold surface occurs very rapidly.

The time needed for the frequency decrease to reach a plateau is dependent on the concentration of $AsMo_{11}VO_{40}^{4-}$ in solution. The higher concentration of $AsMo_{11}VO_{40}^{4-}$ anions in solution, the faster the frequency decreases. In this work, in the concentration range (0.05−10 mM) employed, the time needed for reaching the plateau did not exceed 800 s. Figure 2A represents the amount of frequency difference measured at the plateau as a function of $AsMo_{11}VO_{40}^{4-}$ concentration in solution. It indicates that the adsorption amount of $AsMo_{11}VO_{40}^{4-}$ anion on gold surface is saturated and independent of the bulk concentration as long as its bulk concentration is above 1 mM.

The overall frequency change is around 54 Hz when the $AsMo_{11}VO_{40}^{4-}$ bulk concentration is above 1 mM. According to the Sauerbrey equation, the frequency change 54 Hz corresponds to a surface coverage of $1.7 \times 10^{-10}$ mol $cm^{-2}$ which indicates a monolayer of $AsMo_{11}VO_{40}^{4-}$ anion formed on the gold surface, because a theoretical coverage of the close-packed monolayer is $1.8 \times 10^{-10}$ mol $cm^{-2}$, assuming 5.3 Å for the radius of $AsMo_{11}VO_{40}^{4-}$ anion (obtained from X-ray crystallographic study).[66−68]

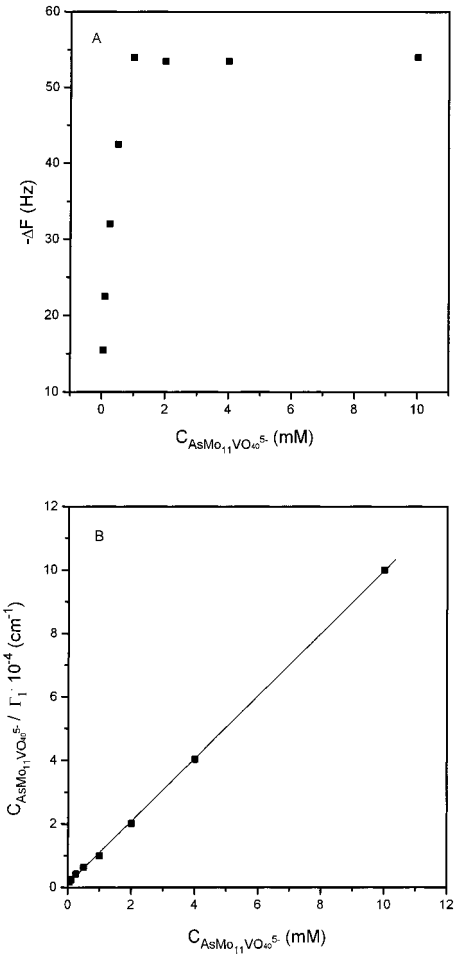


**Figure 2.** (A) Frequency change versus bulk concentration of $AsMo_{11}VO_{40}^{4-}$ anions and (B) data calculated from A plotted according to the Langmuir equation (eq 2).

The data in Figure 2A can be further described using the Langmuir adsorption isotherm which is expressed by the following equation:

$$C/\Gamma_1 = (1/K\Gamma_{max}) + C/\Gamma_{max} \qquad (2)$$

Where $C$ is the bulk concentration of $AsMo_{11}VO_{40}^{4-}$ anion in the solution, $\Gamma_1$ is the calculated coverage based on the frequency change at the plateau region, $\Gamma_{max}$ is the maximum coverage, and $K$ is the adsorption equilibrium constant. Figure 2B represents the plot drawn for the value of $C/\Gamma_1$ versus $C$. Obviously the plots exhibit a linear relationship between the two parameters. Although a good fit of experimental data to Langmuir equation does not prove that the system obeys the assumptions of the Langmuir model, it is reasonable to extract the maximum coverage, $\Gamma_{max}$, from the slope of the $C/\Gamma_1$ versus $C$ plot. Here, a $\Gamma_{max}$ of $1.7 \times 10^{-10}$ mol $cm^{-2}$ is obtained, which corresponds to the coverage of a close-packed monolayer of $AsMo_{11}VO_{40}^{4-}$ anion.

The interpretation of the intercept of the plot in Figure 2B in view of eq 2 can give the adsorption equilibrium constant, $K = 3.7 \pm 0.1 \times 10^3$ L $mol^{-1}$ in the adsorption course. The free energy of adsorption at infinite dilution ($\Delta G°_{ads}$) is estimated from the value of $K$ by invoking the relation of $\Delta G°_{ads} = -RT \ln K$. The $\Delta G°_{ads}$ value can be determined to be −20 kJ/mol which is slightly less than that of alkanethiol adsorbed on Au surface.[69] This indicates

(66) Keggin, J. F. *Nature* **1934**, *144*, 75.
(67) Izumi, Y.; Hasebe, R.; Urabe, K. *J. Catal.* **1983**, *94*, 402.
(68) Highfield, J. G.; Moffat, J. B. *J. Catal.* **1984**, *88*, 177.
(69) Karpovich, D. S.; Blanchard, G. J. *Langmuir* **1994**, *10*, 3315.

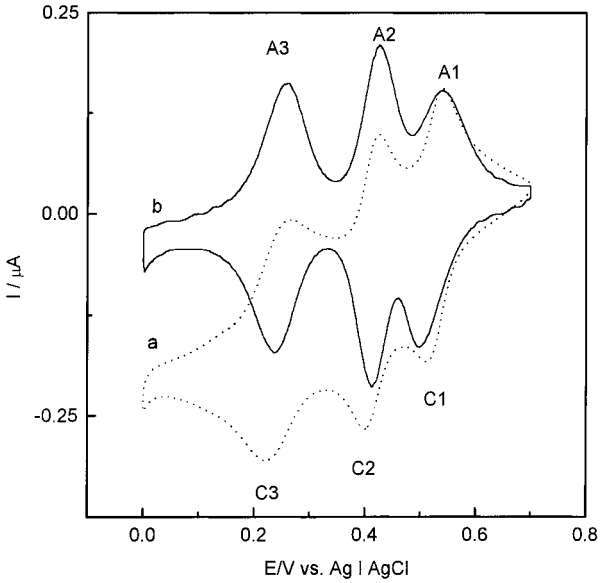


**Figure 3.** (a) Cyclic voltammogram of the Au electrode in 1 mM $AsMo_{11}VO_{40}^{4-}$ in 0.1 M $HClO_4$ and (b) cyclic voltammogram of the $AsMo_{11}VO_{40}^{4-}$ SAM on Au electrode in 0.1 M blank $HClO_4$. Scan rate: 100 mV $s^{-1}$.

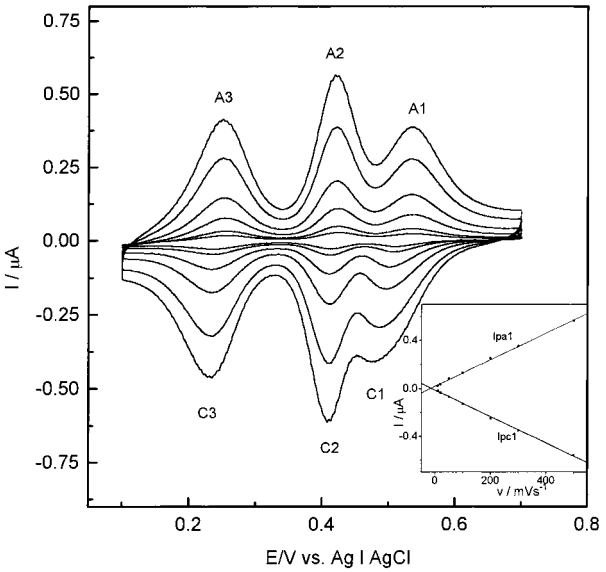


**Figure 4.** Cyclic voltammogram of the $AsMo_{11}VO_{40}^{4-}$ SAM on Au electrode in 0.1 M blank $HClO_4$ at different scan rates. The inset shows variation of the cathodic and anodic current with scan for A1/C1 peak.

that the adsorption of the $AsMo_{11}VO_{40}^{4-}$ anions on gold surface is very favorable.

**2. Characterization of the $AsMo_{11}VO_{40}^{4-}$ SAM on Gold.** The SAM of $AsMo_{11}VO_{40}^{4-}$ anion was prepared by immersing gold surface into 0.1 M $HClO_4$ solution containing 10 mM $AsMo_{11}VO_{40}^{4-}$ anion for 3 h. The gold substrate was then removed and rinsed thoroughly with 0.1 M $HClO_4$ solution.

*2.1. Electrochemistry of the SAM of $AsMo_{11}VO_{40}^{4-}$ Anion on Gold.* Because polyoxometalates have good redox activity and are extensively used as the electrocatalysts, the electrochemical method is chosen to characterize the property of $AsMo_{11}VO_{40}^{4-}$ SAM.[70]

Curve a in Figure 3 represents the first cyclic voltammogram of bare gold electrode just after immersed into 0.1 M $HClO_4$ solution containing 1 mM $AsMo_{11}VO_{40}^{4-}$ anion. In the potential range of between 0.7 and 0.0 V, the $AsMo_{11}VO_{40}^{4-}$ anion exhibits three-step redox waves with the midpoint potentials $E_{mid}$ of 0.525, 0.405, and 0.529 V, where $E_{mid} = (E_{pa} + E_{pc})/2$; $E_{pa}$ and $E_{pc}$ are the cathodic and anodic peak potential. Coulometric studies showed that each reduction corresponded to a two-electron transfer.[71] Moreover, the potentials at which the reduction occurred were dependent on solution pH, indicating that a change in the extent of protonation of the anion occurred upon reduction. In the range of pH < 4.0, as the pH increases, the shapes of redox peaks keep unchanged, and the $E_{mid}$ of all three redox couples shift −60 mV/pH, close to the theoretical value −60 mV/pH for $2e^-/2H^+$, confirming that the addition of two $H^+$ to the two-electron reduction.[71] So the three pairs of redox peaks C1/A1, C2/A2, and C3/A3 represent the redox reaction of $AsMo_{11}VO_{40}^{4-}/H_2AsMo_{11}VO_{40}^{4-}$, $H_2AsMo_{11}VO_{40}^{4-}/H_4AsMo_{11}VO_{40}^{4-}$, and $H_4AsMo_{11}VO_{40}^{4-}/H_6AsMo_{11}VO_{40}^{4-}$. It is also observed that when pH ≥ 4.0, the anion was hydrolytically unstable and the oxidation−reduction was no longer reversible.

Curve b in Figure 3 further shows the cyclic voltammogram of $AsMo_{11}VO_{40}^{4-}$ SAM on gold electrode in 0.1 M blank $HClO_4$ solution in the same potential range. As can be observed, the $AsMo_{11}VO_{40}^{4-}$ SAM shows better electrochemical response (curve b) than the solution containing $AsMo_{11}VO_{40}^{4-}$ anions (curve a). It is noteworthy that for three redox couples of the $AsMo_{11}VO_{40}^{4-}$ SAM the surface formal potential $E°'_{sur}$ ($E_{mid} = (E_{pa} + E_{pc})/2$) is 0.52, 0.41, and 0.25, which is almost the same as that for the solution containing $AsMo_{11}VO_{40}^{4-}$ anions on a bare gold electrode. This feature is consistent with the first-order predictability of formal potentials generally observed for immobilized molecules.[72]

Figure 4 illustrates the cyclic voltammograms of $AsMo_{11}VO_{40}^{4-}$ SAM on gold electrode in 0.1 M $HClO_4$ at various scan rates. The three pairs of peaks C1/A1, C2/A2, and C3/A3 all show the feature of reversible surface redox behavior at all scan rates examined ($v \leq 300$ mV $s^{-1}$). The cathodic peak currents ($i_{pc}$) and anodic peak currents ($i_{pa}$) of the three pairs as a function of $v$ were linear ($r = 0.999$) with zero intercept (the inset in Figure 4 shows the $i_{pc}$ and $i_{pa}$ as a function of $v$ for C1/A1 redox peak). For every pair of peaks its $i_{pc}$ and $i_{pa}$ are equal at each scan rate. However, the peak potential separations of the three pairs $\Delta E_p$ is < 35 mV instead of the value zero expected for a reversible surface redox process occurring.[73] These small potential separations, which might be attributed to a nonideal behavior of the adsorbed moieties,[73−75] are common to all electrodes coated at the monolayer and submonolayer level.[76]

The surface coverage of $AsMo_{11}VO_{40}^{4-}$ anions on gold electrode can be also calculated according to the equation as

$$\Gamma_0 = Q/nFA \qquad (3)$$

Where $\Gamma_0$, $Q$, and $A$ represent the surface coverage of the redox species (mol $cm^{-2}$), quantity of electric charge ($C$) and electrode area ($cm^2$) measured with $Fe(CN)_6^{3-/4-}$, and $Q$ can be obtained by integration of the redox peaks of the voltammograms. For every peak of all three pairs their

(70) Sadakane, M.; Steckhan, E.*Chem. Rev.* **1998**, *98*, 219.
(71) Liu, S.; Tang, Z.; Dong, S.; Wang, E. Manuscript in preparation.
(72) Lenhard, J. R.; Roclin, R.; Abruna, H.; Willman, K.; Kuo, K.; Nowak, R.; Murray, R. W. *J. Am. Chem. Soc.* **1978**, *100*, 5213.
(73) Brown, A. P.; Anson, F. C. *Anal. Chem.* **1977**, *49*, 1589.
(74) Smith, D. F.; Willman, K.; Kuo, K.; Murray, R. W. *J. Electroanal. Chem.* **1979**, *95*, 217.
(75) Ilangovan, G.; Pillai, K. C. *Langmuir* **1997**, *13*, 566.
(76) Facci, J. S. *Langmuir* **1987**, *3*, 525.

*Q* values are almost equal. It demonstrates that the adsorbed amounts on gold surface are unchanged for various redox forms of $AsMo_{11}VO_{40}^{4-}$ anion ($AsMo_{11}VO_{40}^{4-}$, $H_2AsMo_{11}VO_{40}^{4-}$, $H_4AsMo_{11}VO_{40}^{4-}$, and $H_6AsMo_{11}VO_{40}^{4-}$). Because the electrochemical measurements are done in 0.1 M $HClO_4$ blank solution, it can be concluded that the $AsMo_{11}VO_{40}^{4-}$ SAM is not desorbed from gold electrode surface even when its redox form has been changed. It also shows that the $AsMo_{11}VO_{40}^{4-}$ SAM can firmly be adsorbed on gold surface. The surface coverage of $AsMo_{11}VO_{40}^{4-}$ SAM on gold electrode is estimated to be $1.78 \times 10^{-10}$ mol cm$^{-2}$ which corresponds to a monolayer coverage and also is in good agreement with the QCM results.

The $AsMo_{11}VO_{40}^{4-}$ SAM on gold electrode showing three pairs of reversible peaks is different from that of the $SiW_{12}O_{40}^{4-}$ SAM on silver electrode.[48−50] The cyclic voltammogram of the $SiW_{12}O_{40}^{4-}$ SAM on silver electrode in 0.1 M $HClO_4$ indicates that the electrode is passivated over a wide range of potential (up to 2 V). Besides, the electrochemical behavior of $AsMo_{11}VO_{40}^{4-}$ SAM on gold electrode is also different from that of $SiW_{12}O_{40}^{4-}$ anions adsorbed on gold electrode.[48,77] Various redox forms of $AsMo_{11}VO_{40}^{4-}$ anions are all adsorbed strongly on gold electrode at a monolayer level, whereas the reduced form of $SiW_{12}O_{40}^{4-}$ anions tends to be desorbed from the Au electrode surface determined by QCM.[77] Obviously the $AsMo_{11}VO_{40}^{4-}$ SAM strongly adsorbed on gold surface can well exert the redox catalytic activity of polyoxometalates, which is beneficial to construction of functional surface.[70]

After the $AsMo_{11}VO_{40}^{4-}$ SAM on gold electrode is placed in air for 15 days or in an electrolyte solution for a week, its cyclic voltammograms (including peak current and peak potential) do not change upon cycling. It shows that the $AsMo_{11}VO_{40}^{4-}$ SAM has high stability both in air and in liquid.

The adsorption of polyoxometalate on electrode surfaces has been extensively studied by Anson's group through electrochemical measurement.[78−80] They find that the monolayer quantities of the polyoxometalate anion is irreversibly and strongly adsorbed on electrode surface. However, its structure on electrode surface remains unclear.

*2.2. In-Situ STM.* Scanning tunneling microscopy (STM) has extensively been applied to characterize molecular structure of organic SAM[81] and it also gives an opportunity to observed the microscopic arrangement of polyoxometalates on substrate.[82−88] Due to the requirement of an atomically flat surface for STM image, a Au(111) facet, replacing the polycrystalline gold substrate, was chosen as imaging substrate in STM experiment.[89,90] The $AsMo_{11}VO_{40}^{4-}$ SAM on single-crystal Au(111) electrode (prepared according to Clavilier's method[65]) exhibits similar voltammetric behavior as that on the gold electrode, and its coverage on Au(111) electrode determined by electrochemical method also corresponds to a close-packed monolayer. Figure 5A shows a typical macro-scale STM image of the $AsMo_{11}VO_{40}^{4-}$ SAM on Au(111) surface in 0.1 M $HClO_4$ blank solution without applying potential. The SAM surface consists of atomically flat terrace-step structures and no domain structures or aggregates can be observed even at the edge of step. It strongly suggests that the $AsMo_{11}VO_{40}^{4-}$ SAM is homogeneously adsorbed on Au(111) without forming partial multilayers or aggregates. After the SAM on Au(111) is immersed into electrolyte solution for a week or exposed to air for 15 days, STM images demonstrate that the $AsMo_{11}VO_{40}^{4-}$ SAM is still very uniform and smooth and no aggregates occur. The results also indicate that the $AsMo_{11}VO_{40}^{4-}$ SAM has good stability. When we try to image the $AsMo_{11}VO_{40}^{4-}$ SAM at the atomic level, no clear high-resolution image of either the $AsMo_{11}VO_{40}^{4-}$ anion or Au atom can be observed.

To gain further infomation on the structure of the $AsMo_{11}VO_{40}^{4-}$ SAM on Au(111), in-situ STM images were acquired by applying a potential of +0.7 V (vs Ag|AgCl). Large-frame STM shows that the well-defined terrace-step is easily observed and the $AsMo_{11}VO_{40}^{4-}$ SAM is also very uniform and smooth (as shown in Figure 5B). Figure 5C shows the typical raw high-resolution STM image of $AsMo_{11}VO_{40}^{4-}$ SAM on Au(111). The inset (upper right) shows the two-dimensional Fourier spectrum of the image, in which the 4-fold symmetry spots are seen. Different from the images obtained without applying potential, Figure 5C represents a clear two-dimensional ordered array. In Figure 5C, the molecular rows along the arrows *a* and *b* cross each other at 90°, and the intermolecular distances along these directions are almost equal to each other and are found to be about 10−11 Å. On the basis of the orientation of molecular row and the intermolecular distance, it is concluded that the $AsMo_{11}VO_{40}^{4-}$ SAM is composed of square unit cells. A $D_{2d}$ symmetric array with 2.8 Å van der Waals oxygen−oxygen contacts between nearest-neighbor anions leads to a 10.4 Å separation between anions, which is consistent with our experimental value. The arrangement observed for the $AsMo_{11}VO_{40}^{4-}$ SAM on Au(111) at +0.7 V is also similar to Gewirth's report of $SiW_{12}O_{40}^{4-}$ SAM on Ag(111).[48] The lattice spaces, 10−11 Å, are just equal to the dimension of polyoxometalate obtained from X-ray crystallographic study,[66−68] which shows the $AsMo_{11}VO_{40}^{4-}$ SAM on Au(111) is a close-packed array. The STM image also indicates a surface coverage of the $AsMo_{11}VO_{40}^{4-}$ SAM on Au(111) to be around $1.8 \times 10^{-10}$ mol cm$^{-2}$, which is consistent with that estimated from QCM and electrochemical data.

Why do we choose +0.7 V as the potential of studying high-resolution STM images of the $AsMo_{11}VO_{40}^{4-}$ SAM? Two factors must be considered: (1) in fact, during STM imaging the STM tip can greatly affect the quality of images.[91−93] Previous investigations in which the STM tip force was measured simultaneously with tunneling have shown that these forces can be hundreds of nanonewtons for nanoampere tunneling currents, resulting in both elastic deformations of sample surface and molecular movements of alkanethiol SAM.[94−96] Especially, in our

(77) Keita, B.; Nadjo, L.; Belanger, D.; Wilde, C. P.; Hilaire, M. *J. Electroanal. Chem.* **1995**, *384*, 155.
(78) Rong, C.; Anson, F. C. *Anal. Chem.* **1994**, *66*, 3124.
(79) Rong, C.; Anson, F. C. *Inorg. Chim. Acta* **1996**, *242−243*, 1.
(80) Kuhn, A.; Anson, F. C. *Langmuir* **1996**, *12*, 5481.
(81) Poirier, G. E. *Chem. Rev.* **1997**, *97*, 1117.
(82) Keita, B.; Nadjo, L.; Kjoller, K. *Surf. Sci.* **1991**, *256*, L613.
(83) Watson, B. A.; Barteau, M. A.; Haggerty, L.; Lenhoff, A. M.; Weber, R. S. *Langmuir* **1992**, *8*, 1145.
(84) Keita, B.; Chauveau, F.; Theobald, F.; Belanger, D.; Nadjo, L. *Surf. Sci.* **1992**, *264*, 271.
(85) Zhang, B.; Wang, E. *J. Electroanal. Chem.* **1995**, *388*, 207.
(86) Song, I. K.; Kaba, M. S.; Coulston, G.; Kourtakis, K.; Barteau, M. A. *Chem. Mater.* **1996**, *8*, 2352.
(87) Song, I. K.; Kaba, M. S.; Barteau, M. A. *J. Phys. Chem.* **1996**, *100*, 17528.
(88) Klemperer, W. G.; Wall, C. G. *Chem. Rev.* **1998**, *98*, 297.
(89) Hayes, W. A.; Kim, H.; Yue, X.; Perry, S. S.; Shannon, C. *Langmuir* **1997**, *13*, 2511.
(90) Zamborini, F. P.; Crooks; R. M. *Langmuir* **1998**, *14*, 3279.
(91) Bengel, H.; Cantow, H.-J.; Maganov, S. N.; Monconduit, L.; Evain, M.; Whangbo, M.-H. *Surf. Sci.* **1994**, *321*, L170.
(92) Bengel, H.; Cantow, H.-J.; Maganov, S. N.; Hillebrecht, H.; Thiele, G.; Liang, W.; Whangbo, M.-H. *Surf. Sci.* **1995**, *343*, 95.
(93) Bengel, H.; Cantow, H.-J.; Evain, M.; Maganov, S. N.; Monconduit, L.; Whangbo, M.-H. *Surf. Sci.* **1996**, *365*, 461.

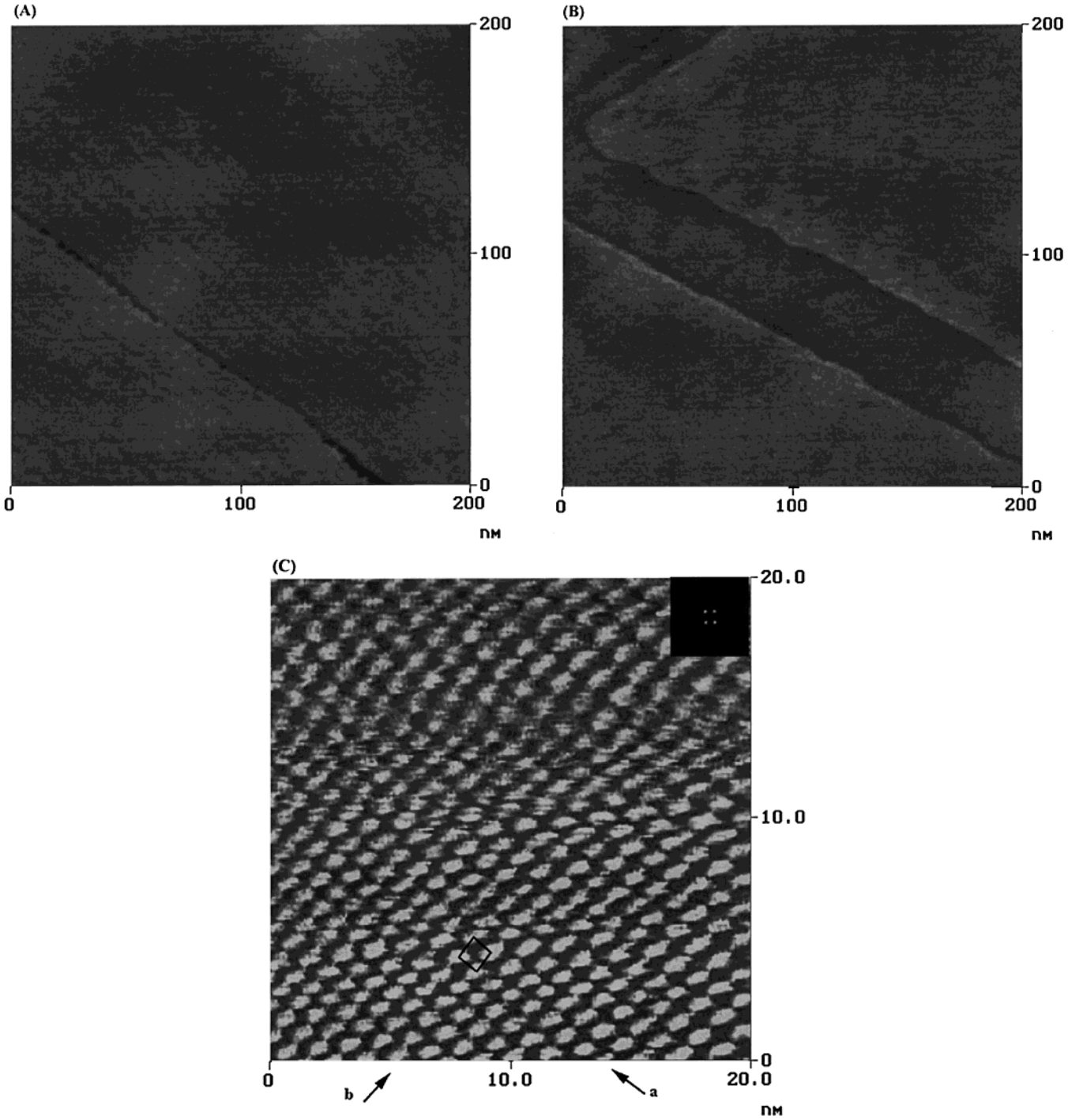


**Figure 5.** (A) Typical large-scale STM image (200 × 200 $nm^2$ area) of the $AsMo_{11}VO_{40}^{4-}$ SAM on Au(111) surface in 0.1 M blank $HClO_4$ without applying potential; (B) typical large-scale STM image (200 × 200 $nm^2$ area) of the $AsMo_{11}VO_{40}^{4-}$ SAM on Au(111) surface in 0.1 M blank $HClO_4$ at +0.7 V; and (C) typical atomic resolution STM image (20 × 20 $nm^2$ area) of the $AsMo_{11}VO_{40}^{4-}$ SAM on Au(111) surface in in 0.1 M blank $HClO_4$ at +0.7 V. Tunneling current = 1 nA; tip bias = 100 mV. The Fourier spectrum of raw data are shown as the inset.

study, the repulsive interaction between the adsorbed charged $AsMo_{11}VO_{40}^{4-}$ anions can further impede the acquisition of the clear high-resolution STM images without applying potential. In contrast, when the potential of +0.7 V is applied, the Au(111) surface possesses many positive charges (the potential of zero charge for Au(111) is +0.32 V vs Ag|AgCl).[97,98] Because the positive charges of Au(111) surface can strongly attract the opposite charges of $AsMo_{11}VO_{40}^{4-}$ anions and weaken the repulsive interaction between the adsorbed $AsMo_{11}VO_{40}^{4-}$ anions, it can improve the strength of the $AsMo_{11}VO_{40}^{4-}$ SAM and prevent the influence caused probably by STM tip. So a clear high-resolution STM image of the $AsMo_{11}VO_{40}^{4-}$ SAM can be obtained. (2) According to the electrochemical measurement, there is no redox reaction of the $AsMo_{11}$-

(94) Mate, C. M.; Erlandsson, R.; McClelland, G. M.; Chiang, S. *Surf. Sci.* **1989**, *208*, 473.
(95) Salmeron, M.; Ogletree, D. F.; Ocal, C.; Wang, H.-C.; Neubauer, G.; Kolbe, W.; Meyers, G. *J. Vacuum Sci. Technol. B* **1991**, *9*, 1347.
(96) Touzov, I.; Gorman, C. B. *J. Phys. Chem. B* **1997**, *101*, 5263.
(97) Lipkowski, J.; Stolberg, L. In *Adsorption of molecules at metal electrode*; Lipkowski, J., Ross, P. N., Eds.; VCH: New York, 1992; p 171.
(98) Bizzotto, D.; Lipkowski, J. *Prog. Collid Polym. Sci.* **1997**, *103*, 201.

$VO_{40}^{4-}$ SAM occurring above +0.7 V. In other words, the $AsMo_{11}VO_{40}^{4-}$ anions adsorbed on Au surface are also on the highest oxidation state at +0.7 V and remain the form of the $AsMo_{11}VO_{40}^{4-}$ anions.

Future work will be done to obtain the detailed molecular arrangement of the $AsMo_{11}VO_{40}^{4-}$ SAM without applying potential and, therefore, eliminating the molecular rearrangements might have happened during the application of potential. Moreover, besides (111) oriented surfaces, the polycrystalline gold also consists of (110) and (100) oriented surfaces, so the detailed molecular arrangement of $AsMo_{11}VO_{40}^{4-}$ SAM on these surfaces should be observed in future wok.

## Conclusion

We have demonstrated that a new kind of inorganic monolayer can be formed by self-assembly of $AsMo_{11}VO_{40}^{4-}$ anions onto a gold surface. The formation, structures, and properties of the $AsMo_{11}VO_{40}^{4-}$ SAM are studied by QCM, electrochemistry, and in-situ STM. QCM measurements show that the self-assembly process is a very fast process and the adsorption is very favorable. Moreover, the maximum surface coverage of $AsMo_{11}VO_{40}^{4-}$ SAM can be calculated corresponding to a monolayer coverage and does not depend on solution concentration of the species. In-situ STM images reveal that the $AsMo_{11}VO_{40}^{4-}$ SAM is very uniform and smooth, and no aggregates or domain structures appear even after the SAM is placed in an electrolyte solution for 7 days or in air for 15 days. In electrochemical experiments, the peak current of the $AsMo_{11}VO_{40}^{4-}$ SAM also remains unchanged after the SAM is exposed in air or solution for such a long time. Both results imply that the new kind of inorganic SAM, which is not decomposed in air or desorbed in solution, has good stability and resistance to environmental attack.

Furthermore, electrochemical measurements prove that the $AsMo_{11}VO_{40}^{4-}$ SAM on gold electrode maintains the same formal potential and exhibits better redox behavior compared with the $AsMo_{11}VO_{40}^{4-}$ anions in the solution, which is very favorable for electrocatalytical reaction of the polyoxometalate anions.[70,71] So we can anticipate that the self-assembly of a homogeneous, molecular oxidation catalyst on electrode surfaces will be carried out to create a new class of single-site heterogeneous electrocatalyst. In addition, the polyoxometalate SAMs will probably be extensively used in solid-state devices, photo- and electrochromic displays, and fuel cells as a good electron-transfer reagent.[58−60] Obviously, it is feasible that the special functional material will be constructed through fabricating the SAMs of various inorganic molecules in the future.

**Acknowledgment.** This work has been supported by the National Natural Science Foundation of China. We thank Professor Enbo Wang (Department of Chemistry, Northeast Normal University) for synthesizing the polyoxometalate samples.

LA9907127